

## Thermomechanical stability and integrability of an embedded ceramic antenna with an integrated sensor element for wireless reading in harsh environments

This content has been downloaded from IOPscience. Please scroll down to see the full text.

2013 J. Phys.: Conf. Ser. 476 012055

(<http://iopscience.iop.org/1742-6596/476/1/012055>)

View [the table of contents for this issue](#), or go to the [journal homepage](#) for more

Download details:

IP Address: 130.238.88.148

This content was downloaded on 20/10/2014 at 12:40

Please note that [terms and conditions apply](#).

## Thermomechanical stability and integrability of an embedded ceramic antenna with an integrated sensor element for wireless reading in harsh environments

P. Sturesson<sup>1,2,3</sup>, Z. Khaji<sup>2</sup>, S. Knaust<sup>2</sup>, J. Sundqvist<sup>1,2</sup>, L. Klintberg<sup>2</sup>, and G. Thornell<sup>1,2</sup>

<sup>1</sup>Ångström Space Technology Centre, Dept. of Eng. Sciences, Uppsala University, Uppsala, Sweden

<sup>2</sup>Division of Microsystems Technology, Dept. of Eng. Sciences, Uppsala University, Uppsala, Sweden

<sup>3</sup>Swedish National Defence College, Stockholm, Sweden

Corresponding author: peter.sturesson@angstrom.uu.se

This paper reports on the design, manufacturing and evaluation of a small, wirelessly powered and read resonating antenna circuit with an integrated pressure sensor. The work aims at developing miniature devices suitable for harsh environments, where high temperature prevents the use of conventional, silicon-based microdevices. Here, the device is made of alumina with platinum as conducting material. Ceramic green tapes were structured using high-precision milling, metallized using screen printing, and subsequently laminated to form stacks before they were sintered. The device's frequency shift as a function of temperature was studied up to 900°C. The contributions to the shift both from the thermomechanical deformation of the device at large, and from the integrated and, so far, self-pressurized sensor were sorted out. A total frequency shift of 3200 ppm was observed for the pressure sensor for heating over the whole range. Negligible levels of thermally induced radius of curvature were observed. With three-point bending, a frequency shift of 180 ppm was possible to induce with a curvature of radius of 220 m at a 10 N load. The results indicate that a robust pressure sensor node, which can register pressure changes of a few bars at 900°C and wirelessly transmit the signal, is viable.

### 1. Introduction

Miniature devices for harsh environments are facing an increasing interest. Applications are found in, e.g., space exploration, geothermal research, and monitoring of combustion engines [1, 2]. In harsh environments high temperature, corrosive substances, high pressure and radiation may be confronted. For electronics and sensors, high temperatures can be regarded as a prime challenge.

Above about 600°C there are two main challenges on the generic level: lack of suitable materials and difficulty of interfacing. Beside thermomechanical effects that can jeopardize the operation of the component itself, signal and power transfer by leads becomes a challenge.

Silicon, which may deform slowly at these temperatures if loaded mechanically [3], can be replaced either by Low-Temperature Co-fired Ceramics (LTCC) or by thick film technologies with pre-sintered ceramics [4], or, above 800°C, by High Temperature Co-fired Ceramics (HTCC), which should withstand temperatures well beyond 1000°C [5].

Fonseca, Radosavljevi, Xiong and Tan et al. have demonstrated wireless ceramic two-membrane pressure sensors exhibiting frequency shifts in the range of 1000-10000 ppm per bar [6-9].

Here, the thermomechanical behaviour of a resonant LC antenna circuit made of alumina with printed platinum conductors for use in a sensor node is studied, as this is vital for the design of the device itself, as well as for its integration in physical system architectures. Since the resonance frequency shift should be used for reading of the sensor node's sensor, its dependency on temperature and mechanical deflection is studied.



To demonstrate the integrability with a sensor element, one of the antenna devices has been furnished with a cavity sealed by a metallised membrane, which consists of a capacitor plate to enable wireless pressure readings at high temperatures.

## 2. Design

The antenna is an inductively coupled LC resonance circuit consisting of a multi-turn planar square loop in series with a  $3.6 \times 3.6$  mm, centred capacitor, figure 1 (left). The loop pattern including one capacitor plate is printed on a ceramic substrate, and the second capacitor plate, connected through a via, is printed on the backside, figure 1 (right). The coil conductor width is  $250 \mu\text{m}$  and the substrate thickness is  $250 \mu\text{m}$ .

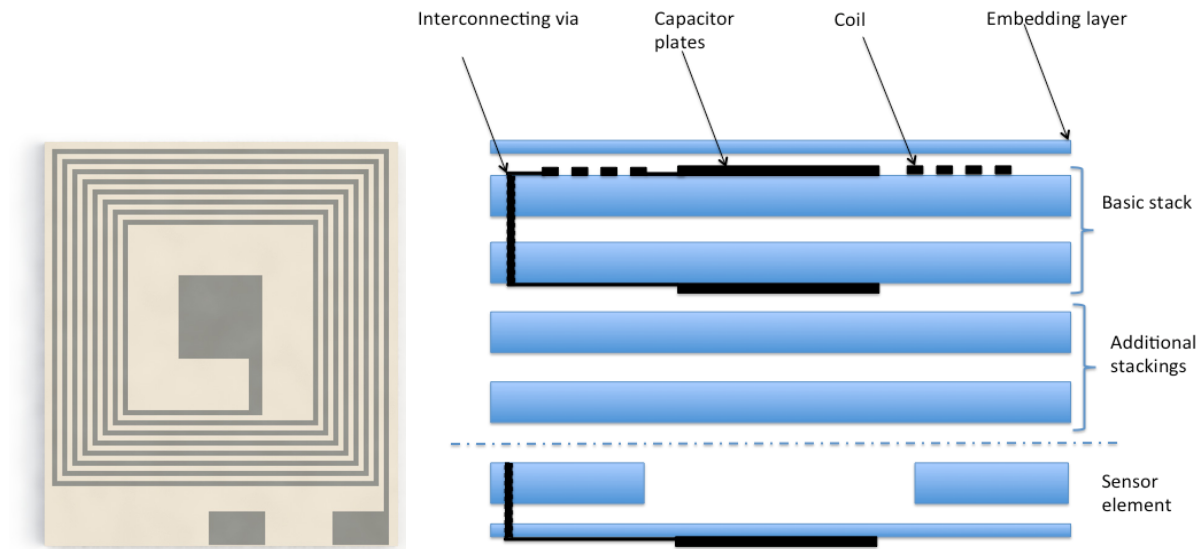


**Figure 1.** Top view of device, showing the antenna LC circuitry (left), and, in cross section, the stacking of the antenna part with sensor element layers and intermediate structural layers (right).

The frequency of the antenna is determined by its inductance,  $L$ , and its capacitance,  $C$ , according to:

$$f = \frac{1}{2\pi\sqrt{LC}}, \quad (1)$$

where the inductance depends on geometry only [10]. The dimensions of the loop are estimated to follow the thermal expansion of the much thicker alumina which amounts to  $0.8\%$  over  $1000^\circ\text{C}$  [11]. The capacitance is given by:

$$C = \epsilon_0 \epsilon_r \frac{A}{d}, \quad (2)$$

where  $A$  is the area of the capacitor plates,  $d$  their spacing,  $\epsilon_0$  the vacuum permittivity, and  $\epsilon_r$  the relative permittivity for alumina. If the thermal expansion can be neglected, the main contribution to the change in resonance frequency will come from changes of the dielectric constant of the substrate. Chen et al. have shown that the dielectric constant of alumina is stable up to  $550^\circ\text{C}$  for  $1 \text{ MHz}$ , after which it starts to increase [12]. The onset temperature for the increase appears to increase with increasing frequency.

Here, with one of the capacitor plates placed on a membrane suspended across a cavity, an increased outside pressure will cause the membrane to deflect, hence change the capacitance and, thereby, the resonance frequency. Similarly, when heating the air inside the cavity, a thermally induced pressure increase will cause the membrane to deflect outwards.

### 3. Materials and fabrication

The devices were laminated from 99.9% 50, 130 and 150  $\mu\text{m}$  thick alumina green tapes (ESL 44007-150/130/50, Electro Science Laboratories, USA). Platinum paste (ESL 5571, ESL Electro Science Laboratories, USA) and a stainless steel screen with a mesh of 325 lines per inch were used for metallization. After printing, the paste was dried at 50°C for 15 minutes.

The pressure sensor element consists of a 130  $\mu\text{m}$  thick sheet with a 5-mm diameter, circular cavity milled with a PCB plotter (Protomat S100, LPKF, Germany) and sealed with a 50  $\mu\text{m}$  thick tape. As a support for the membrane, a 125  $\mu\text{m}$  thick fugitive material (ESL 49000, Electro Sciences Laboratories, USA) was used.

Lamination was performed at 21 MPa and 70°C for 20 minutes in a hydraulic laminator (RMP 210, Bungard, Germany). For devices without sensor elements, the printed sheets were first aligned and laminated in one step, and then laminated with a 50  $\mu\text{m}$  thick top sheet and 4 or 5 150  $\mu\text{m}$  thick sheets from behind. For the device with the sensor element, the sheet with the cavity was laminated with the coil pattern sheet in one step and then laminated with the 50  $\mu\text{m}$  thick embedding and membrane layers (see figure 1). After lamination, the stacks were contoured in the PCB plotter into 23×21 mm devices.

Following a temperature profile with a ramping pace of 1.5°C/min to a dwell temperature of around 500°C to allow the organic binder and fugitive material to dispose, the ramping was increased to 2°C/min to 1550°C where the samples were sintered for two hours.

The resulting devices and their resonance frequencies and thicknesses are presented in table 1.

**Table 1.** Device IDs, total thicknesses, and resonance frequencies.

Device number	Frequency [MHz]	Thickness [ $\mu\text{m}$ ]
1	45	410
2	44	760
3	46	890
4 (w pressure sensor)	63	500

### 4. Characterization

For monitoring the general frequency dependency of the antennas, a small in-house designed and fabricated furnace was used, figure 2. The heat elements were clamped with sintered alumina nitride plates with a centered clearing for the devices to avoid magnetic interferences. An in-house fabricated tunable, 12-cm diameter loop antenna made of a 4-mm diameter copper rod was placed above the furnace, at about 5 cm distance from the devices, and connected to a vector network analyzer (Fieldfox 9923, Agilent, USA). The resonance frequency of active antenna was tuned to the respective device antenna with a variable (5.5-65 pF) capacitor, and an auxiliary 2.5-cm diameter loop antenna, milled from FR-4 PCB, was used to match the impedance to 50  $\Omega$ . The devices were passively powered by the backscattered signal from the active antenna. The network analyzer logged the S11 parameter.

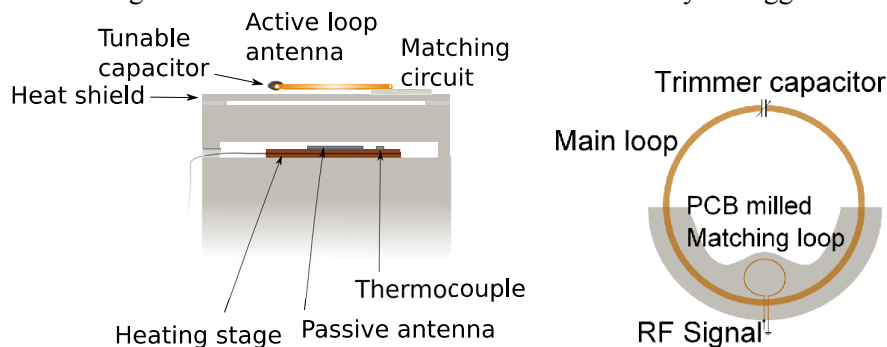


**Figure 2.** Measurement set up (left), with an active loop antenna (right), placed on top of a furnace containing the sample devices. Fans are used to keep the loop antenna below 50°C.

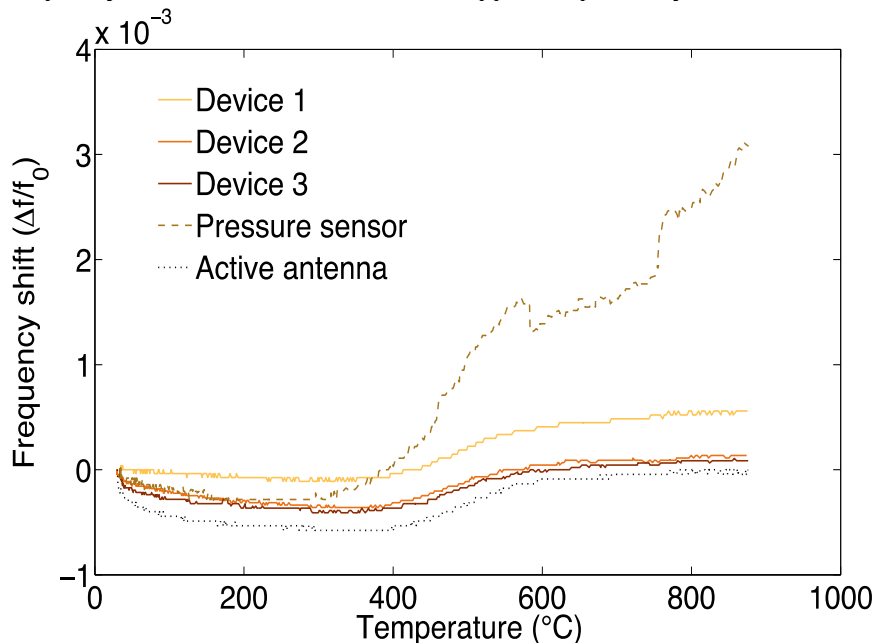
Device 3 was evaluated in a stress meter (FSM 500TC, Frontier Semiconductor, USA) using laser profilometry to measure the thermally induced deflections of the device for temperatures up to 380°C. In addition, the resonance frequency shift was measured on Devices 1, 2 and 3 during three-point bending instrument (AGS-X, Shimadzu, USA) with the load increasing from 0-10 N in steps of 0.5 N.

**5. Results**

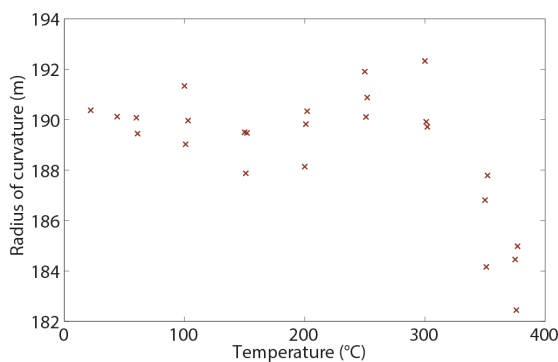
The Q value of the devices, being the ratio of obtained resonance frequency to the 3-dB bandwidth, Table 1, was 6.7 in average with a standard deviation of 0.61.

Figure 3 shows the relative frequency shift of the three antenna devices over a temperature range of room temperature to 900°C. All three follow the same trend, with the frequency decreasing for up to 300°C, then slightly increasing between 400 and 600°C, and finally levelling out above 600°C. This is also the behaviour of the active antenna. The device with the pressure sensor element (No 4) exhibits an additional frequency shift of, in total, 3200 ppm, from 300°C to 900°C.

The thermally induced radius of curvature changed from 190 to 182 m for Device 3, figure 4. No frequency shift could be resolved for this sample in the bending tests, figure 5. For Devices 1 and 2, however, the frequency shows a shift of -80 and -180 ppm, respectively.



**Figure 3.** Frequency shift versus temperature for Devices 1-4 and the active, loop antenna.



**Figure 4.** Radius of curvature versus temperature for Device 3.

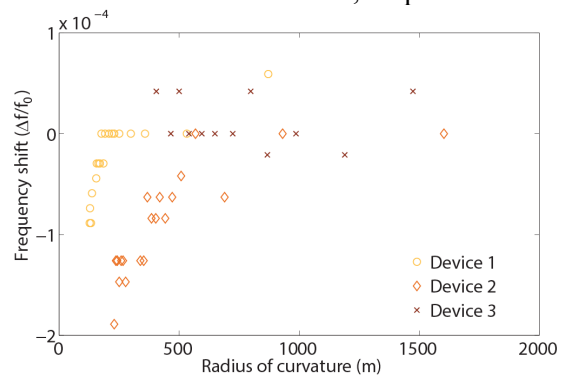


**Figure 5.** Frequency shift versus radius of curvature during three-point bending deformation of Devices 1-3.

## 6. Discussion & Conclusions

The similar behavior of Devices 1-3 and the active antenna, figure 3, suggests that the drift of the active antenna dominates. This effect could be attributed to the large bandwidth of the passive antennas, which makes the detection of small changes more difficult. In general, planar spiral loops have low Q values [13]. This can be improved by choosing a material with higher conductance than platinum, for instance silver or tungsten. They would, however, require a completely different manufacturing concept.

Throughout all these measurements, including the active antenna measurement, an increased frequency shift is observed between 400 and 600°C. This is believed to be caused by a sudden increase in conductivity of the AlN used in the furnace because of impurities, as reported by [14].

The thermally induced radius of curvature observed is very small, figure 4, even considering the relatively large change above 300°C, implying that the ceramic laminate manufacturing scheme provides thermomechanically rather robust components - at least when these are thick. Whether or not this holds also for thinner devices or if the amount of metallization or cavities and membranes is increased, remains to be investigated.

As for the three-point bending, which spans a much larger range of curvature, figure 5, the frequency shift is an order of magnitude smaller than that of the sensor-containing device, implying that these devices may be subjected to significant deformation, resulting, e.g., from mounting stresses or thermal mismatch when integrated, without severe performance losses.

The frequency shift of Device 4 is of a magnitude comparable with that of [6-9] and indicates a capacitance change from the thermally induced inner pressure deflecting the sensor's membrane. This device has a thinner membrane than those it is compared with. These, however, have two membranes and a lower Young's modulus. Hence, the result suggests a possible pressure reading at temperatures up to 900°C but the effect needs further investigation.

## References

- [1] Landis GA 2006 *Acta Astronaut* **59** 570-579
- [2] Spang III H A and H Brown 1999 *Control of jet engines* **7** 1043-1059
- [3] Domnich V, Aratyn Y, Waltrand M K, and Gogotsi Y 2008 *Rev. Adv. Mat. Sci.* **17** 33-41
- [4] Khoong L E, Tan Y M and Lam Y C 2010 *J. Eur. Ceram. Soc.* **30** 1973-1987
- [5] Lekholm V, Persson A, Palmer K, Ericson F, and Thornell G 2013, *J. Micromech. Microeng.* **23**
- [6] Fonseca M A, English J M, von Arx M, and Allen M G 2002 *J. Microelectromechanical Systems*, **11** 337-343
- [7] Radosavljevic G J, Zivanov L D, Smetana W, Maric A M, Unger M, and Nad L F 2009 *IEEE Sensors Journal* **9** 1956-1962
- [8] Xiong J, Zheng S, Hong Y, Li J, Wang Y, Wang W, and Tan Q 2013 *J. Zhejiang University-SCIENCE C (Computers & Electronics)* **14** 258-263
- [9] Tan Q, Kang H, Xiong J, Qin L, Zhang W, Li C, Ding L, Zhang X, and Yang M 2013 *Sensors* **13** 9896-9908
- [10] Greenhouse H M 1974 *IEEE Trans. Parts, Hybrids, Packages* **10** 101-109
- [11] Werdecker W and Aldinger F 1984 *IEEE Trans. Compon., Hybrids, Manuf. Technol.* **7** 399-404
- [12] Chen L Y and Hunter G W 2004 *2004 MRS Meeting Boston MRS*
- [13] Sunderajan S M, del mar Hershenson M, Boyd S P, and Lee T H 1999 *IEEE J. Solid-State Circ.* **34** 1419-1424
- [14] Francis R W and Worell W L 1976 *J. Electr. Chem. Soc.* **123** 430-433